SOLUTIONS OF SOME NONLINEAR PARTIAL DIFFERENTIAL EQUATIONS RELEVANT TO METEOROLOGY AND IMPLICATIONS FOR NUMERICAL METHODS

M.J.P. Cullen
Meteorological Office
Bracknell, U.K.

Summary: Stable consistent numerical schemes are known to converge to the solution of partial differential equations assuming that these are smooth. Smooth solutions are not guaranteed for the inviscid equations commonly used in numerical weather prediction. In such cases the choice of artificial viscosity can change the limiting solution as the mesh is refined. Examples discussed include the barotropic vorticity equation and the quasi geostrophic equations, which usually have smooth solutions; and the one-dimensional shallow water equations and the geostrophic momentum equations which can have discontinuous solutions.

1. INTRODUCTION

It is well-known, e.g. Richtmyer and Morton (1967), that the conditions for a finite difference scheme to converge to the solution of a partial differential equation are consistency and stability. However, this argument inherently assumes that the equation has solutions with at least enough derivatives to make the equation well defined. There are a number of examples in computational fluid dynamics where systems of equations used to model physical events have solutions which become discontinuous in a finite time, or even become infinite. These examples usually arise when dissipative effects are neglected, a common approximation in cases where gas flows are being modelled on rather coarse grids. If this happens it is necessary to be careful to define the problem properly before attempting a numerical solution. For example, the equations describing transonic flow of a perfect gas have solutions that become discontinuous at shocks. The differential equations then become meaningless. However, the physical conservation laws for mass, momentum and energy still apply, and can be solved to give a "generalised" solution which may contain jump discontinuities. It can then be shown that such a solution is the limiting solution as the viscosity tends to zero of solutions of the viscous equations. When solving the problem numerically, it is necessary to ensure that the numerical method solves the conservation laws, rather than the partial differential equation derived from them.

In meteorology, this difficulty is usually viewed in Fourier space, as a tendency for smaller and smaller scales to be generated, even though the initial data may only contain large scales. It is thus used as an explanation for the loss of atmospheric predictability (Lorenz (1969)). However, generation

of small scales does not necessarily result in loss of predictability; as, for instance, the motion of shock waves is completely determined by large-scale information. An example of a solution exhibiting a rapid scale collapse is shown in Figs. 1, 2, and 3. The inviscid incompressible three dimensional equations of flow:

$$\begin{aligned} &\frac{d\underline{u}}{dt} + \underline{u}\cdot\nabla\underline{u} + \nabla p = 0 \\ &\nabla \cdot \underline{u} = 0 \qquad \text{in } \Omega \\ &\int \underline{u}\cdot\underline{n}\, dS = 0 \quad \text{on } \partial\Omega \end{aligned} \tag{1.1}$$

are solved in a periodic unit cube Ω with boundary $\partial\Omega$ at $X = \pm 0.5$, $Y = \pm 0.5$, $Z = \pm 0.5$. The initial data contains vorticity along the lines $Y = 0$, $Z = 0.05$ and $X = 0$, $Z = -0.05$ (Fig. 1).

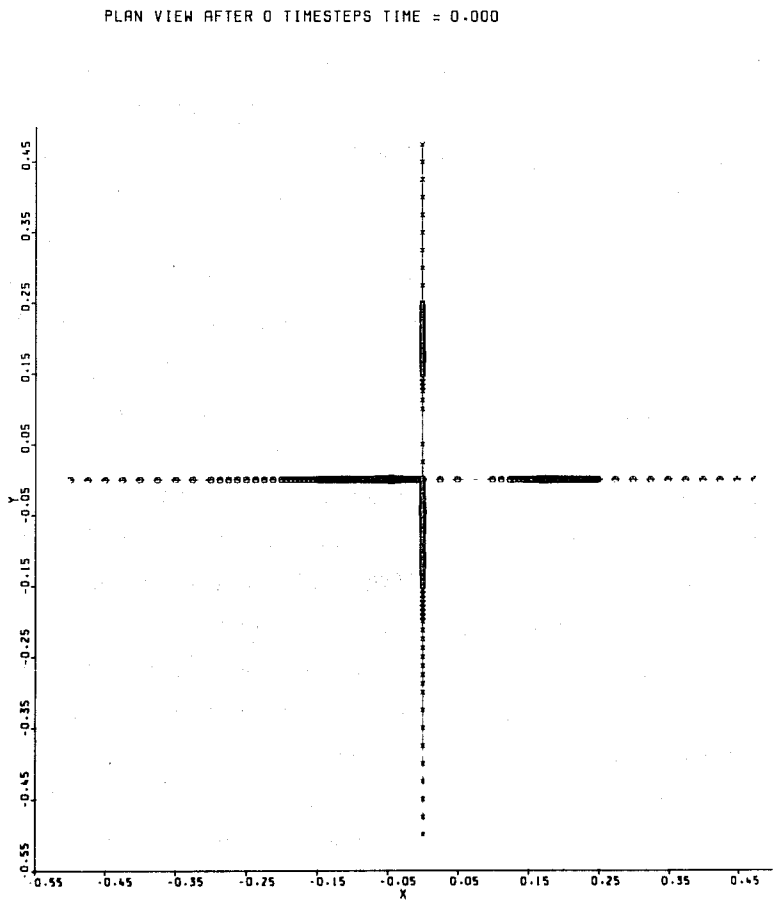

Fig. 1 Initial data for equation (1.1).

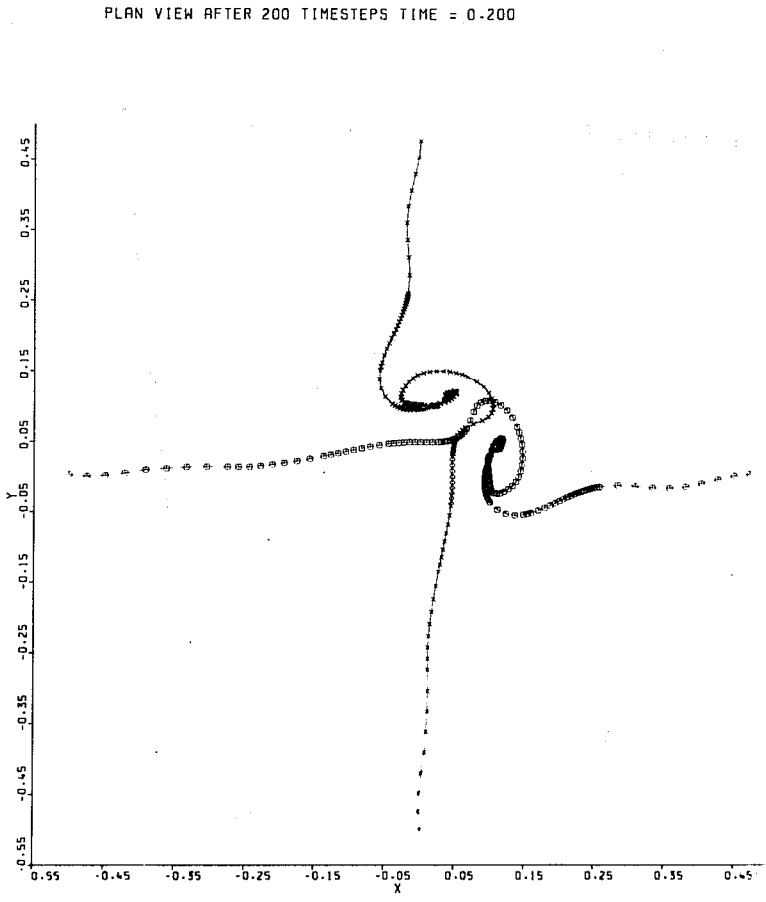

Fig. 2 Solution at t = 0.2.

The solution at t = .2 is shown in Fig. 2, a rapid scale collapse has occurred as the filaments tangle. A graph of the L_1 norm of vorticity, defined by

$$\|\zeta\| = \int |\zeta| \, d\Omega \tag{1.2}$$

is shown in Fig. 3. This evidence shows that it is tending to an infinite value at about t = 0.4.

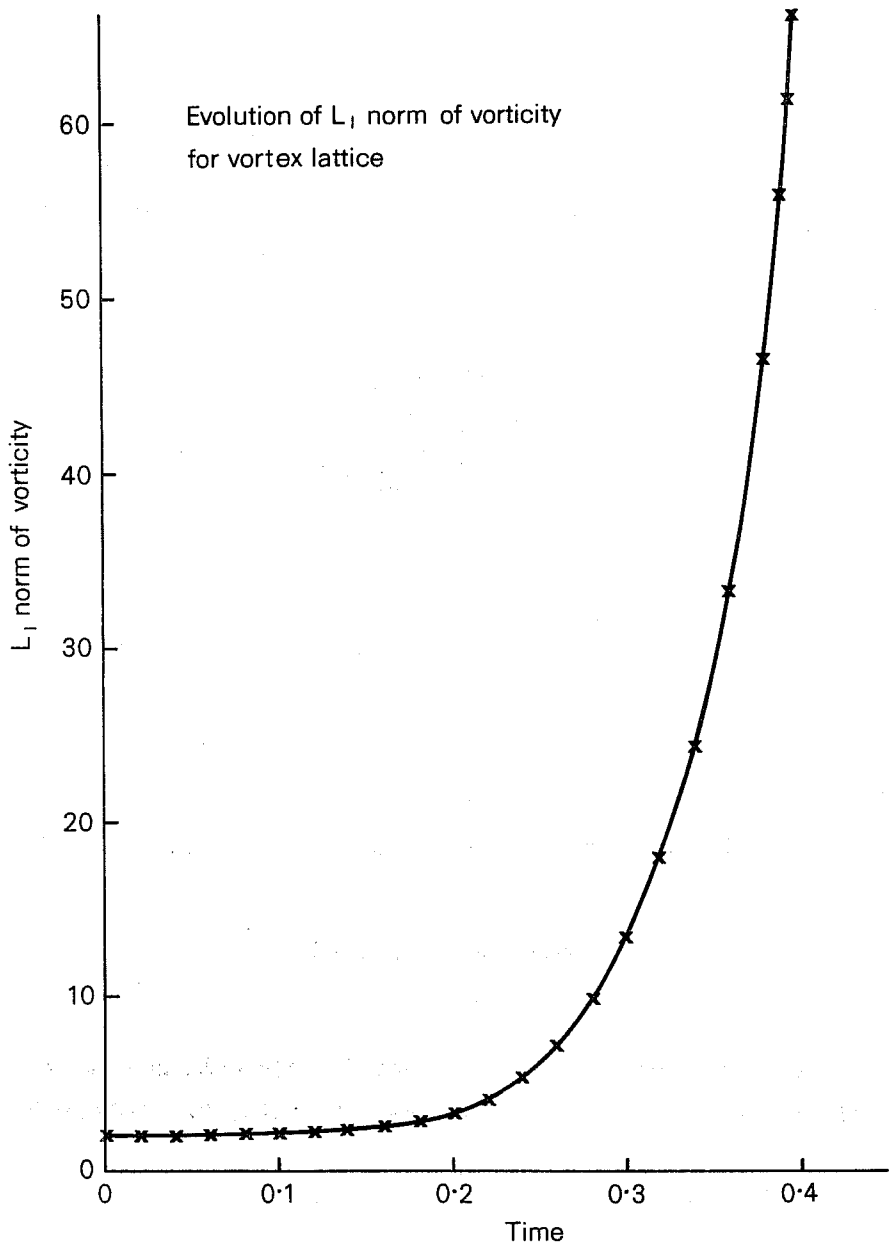

Fig. 3 Plot of the L_1 norm of vorticity against time

This example is still controversial (see Chorin (1981), Brachet et al. (1983)), and it is not yet certain whether infinite vorticity can be produced from smooth initial data in a finite time. If it can, then the inviscid problem (1.1) becomes meaningless and the viscous terms can no longer be neglected. Similarly, a proper numerical solution of (1.1) should also diverge unless viscosity is added. Such divergence is not computational instability, but reflects a genuine property of the equations being modelled.

The problem (1.1) may be a fairly accurate model of what goes on on the smallest scales in the atmosphere. Such rapid generation of small scales is typical of turbulent flows. However, the atmosphere also contains large scale organised flows. It is known that these can be described quite accurately by various approximate systems of equations, using assumptions of hydrostatic and geostrophic balance. In the rest of this paper we consider the properties of these approximate equations, and show that, in several cases, more organised solutions are produced. It is important that the special features of the approximate equations which allow organised solutions are respected by numerical algorithms. If this is not done, the correct large scale organised flow may not be reproduced.

2. QUASI-GEOSTROPHIC EQUATIONS

2.1 The barotropic vorticity equation

One of the simplest approximate equations used to describe meteorological flows is the barotropic vorticity equation. It is obtained by taking the vertical average of the primitive equations, and neglecting the vertically meaned divergence. It gives a reasonable description of the evolution of the 500 mb flow over short periods. The equations are

$$\frac{d\zeta}{dt} + \underline{u}.\nabla(\zeta + f) = 0 \qquad (2.1)$$

where $\underline{u} = \underline{u}(x,y)$ with $\nabla.\underline{u} = 0$

$\zeta = \hat{\underline{k}} \times \nabla \underline{u}$

$\hat{\underline{k}}$ is a unit vector in the vertical

f is the Coriolis parameter.

If the domain Ω in which (2.1) is solved is assumed doubly periodic, then $u(x,y)$ is completely determined by $\zeta(x,y)$ and the condition $\nabla.\underline{u} = 0$. Equation (2.1) states that $(\zeta + f)$ is convected by the wind field $\underline{u}$, but the value of $(\zeta + f)$ cannot be changed following any fluid element. This means that the solution $\zeta(t)$ at any time t can be obtained by a rearrangement of the initial data $\zeta(0)$. All moments of the vorticity:

$$\int \zeta^{\wedge} \, d\Omega \qquad (2.2)$$

are conserved, and the vorticity thus remains bounded indefinitely. It has been proved, by using these facts, that given initial data $\zeta(0)$ of a specified smoothness (i.e. a certain number of derivatives exist), the solution stays this smooth for any arbitrary finite time. Thus discontinuities in ζ cannot be formed in a finite time unless they are present in the initial data (Judovich

(1964), Kato (1967)). This means that standard finite difference schemes will remain consistent, and converge to the correct solution if they are stable.

This theorem, of course, only holds for the approximate set of equations (2.1). However, since these equations are quite accurate for the large scale vertically meaned flow, the theorem helps to explain why a smooth 500 mb flow pattern persists. Any numerical solution of the primitive equations will contain an implied numerical scheme for the barotropic vorticity equation. This scheme should be designed to conserve the moments (2.2). If it does, then it can be proved to be a stable approximation to (2.1) and therefore will converge. However, it is impracticable to conserve all of them in a finite difference calculation on a fixed mesh. The best that can easily be done is to conserve the enstrophy $\int \zeta^2$. Though that does not ensure that $\zeta(t)$ is bounded by its initial values, it does mean that $\zeta(t)$ will stay bounded for all time. This argument was used by Arakawa (1966) and Sadourny (1975) in constructing finite difference schemes which conserve the enstrophy for advection by the non-divergent part of the flow. An advantage of Galerkin methods is that such constraints can naturally be enforced, as in the current ECMWF spectral model.

2.2 The quasi-geostrophic equations

The barotropic vorticity equation cannot describe synoptic developments driven by baroclinic processes. The next set of equations to be considered is the simplest set which does, the quasi-geostrophic equations. In the notation of Pedlosky (1964), these are

$$\Delta_H \psi + \rho^{-1}(\rho \epsilon \psi_z)_z = \omega \tag{2.3}$$

$$u = -\psi_y, \quad v = \psi_x, \quad \theta = \psi_z \tag{2.4}$$

$$\omega_t + u\omega_x + v\omega = -\beta v \quad \text{in } \Omega(x,y)X(0,h)$$

$$\theta_t + u\theta_x + v\theta_y = 0 \quad \text{at } z = 0, h \tag{2.5}$$

$\rho = \rho(z)$, $\epsilon = \epsilon(z)$ are density and stability profiles of a given basic state. ψ is the streamfunction, θ the potential temperature and ω the potential vorticity. β is the northward gradient of the Coriolis parameter. Δ_H is the horizontal Laplacian operater $(\partial^2/\partial x^2 + \partial^2/\partial y^2)$. Initial conditions for (2.3.5) can be specified as values of ω everywhere, and values of θ at $z = 0$ and h. The boundary conditions require care. This is because equations (2.3.5) are derived assuming the Rossby number Ro = U/fL is small, where U and L are typical velocity and length scales. The boundary conditions must be chosen so that they are consistent with a solution with small Ro everywhere.

The solutions of (2.3.5) have been analysed by Bennett and Kloeden (1981a, b). They are essentially determined by advection of the quasi-geostrophic potential vorticity ω eq. (2.4), and the calculation of θ by solving the

Poisson equation (2.3). The boundary conditions for the Poisson equation at $z = 0$, h are the Neuman conditions $\frac{\partial \Psi}{\partial z} = \theta$, with θ determined by (2.5). The simplest boundary conditions in x and y are periodic, rigid wall conditions can be used if additional information is given. If θ is constant at $z = 0$ and h, then Bennett and Kloeden prove that, given smooth initial data, then smooth solutions exist for arbitrary finite times, if $\beta = 0$, or for a finite time proportional to β^{-1} otherwise. They also prove the consistency of the inviscid problem with the inviscid limit of the viscous problem. Thus this case of quasi-geostrophic motion has similar behaviour to the barotropic vorticity equation. If, however, the temperature at $z = 0$ and h is allowed to evolve; then discontinuities may form in θ in a finite time . This would mean that smooth solutions might cease to exist in the interior also. If this happens, the scaling used to derive (2.3.5) will be violated since Ro will be large. Thus the results would not be expected to be physically meaningful.

The theorem proving the existence of smooth solutions depends on the conservation of the quasi-geostrophic potential vorticity following the horizontal non-divergent part of the motion. Thus $\int \omega^n \, d\Omega$ is conserved for all n. If this properly were true for a finite difference approximation it could be proved to be stable and hence convergent. In practice it is **not** conveniently possible to inforce more than the conservation of potential enstrophy, as is done by Arakawa and Lamb (1981).

2.3 Summary

Though schemes satisfying quadratic conservation requirements are favoured by these arguments, and it is almost possible to prove that they converge to the solutions of the simplified equations, all that is required for an approximation to the full primitive equations is that the implied approximation to the simplified equations will remain stable for as long as the scaling assumptions remain valid. This weaker condition is probably satisfied by a much wider range of schemes than just those which conserve enstrophy or potential enstrophy.

3. SHALLOW WATER AND ADVECTION EQUATIONS

3.1 The advection equation

The results of the previous section are essentially based on the advection of vorticity by a two-dimensional nondivergent velocity field. The vorticity stays bounded by its initial values, which in turn implies that the velocity field stays smooth. If the flow is divergent such results no longer hold. The simplest example of this is the one dimensional nonlinear advection equation.

$$\frac{\partial u}{\partial t} + u\frac{\partial u}{\partial x} = 0 \qquad (3.1)$$

The solution of this can easily be obtained, for initial data $u = f(x)$, as

$$u = f(x-ut) \tag{3.2}$$

Equation (3.2) implicitly determines the solution. However, if $f(x)$ is not constant, the solution becomes multi-valued. Suppose $f(0) = u_1, f(1) = u_2$. Then the solution (3.2) at $x = \frac{u_1}{u_1-u_2}$, $t = \frac{1}{u_1-u_2}$ takes both the values u_1 and u_2. For this to happen the solution must become discontinuous, and therefore the differential equation (3.1) is no longer meaningful. It can be given meaning by either adding a dissipative term $\epsilon \partial^2 u/\partial x^2$ to the right-hand side, or by considering instead of (3.1) the conservation law

$$\frac{\partial u}{\partial t} + \frac{\partial}{\partial x}\left(\tfrac{1}{2}u^2\right) = 0 \tag{3.3}$$

Consider the solution of (3.3) for the special initial data

$$\begin{aligned} u &= u_1 \qquad x<0 \\ u &= u_2 \qquad x>0 \end{aligned} \tag{3.4}$$

This is known as the Riemann problem for this equation. Equation (3.3) implies that the rate of change in u in any finite volume of fluid is equal to the net flux $(\frac{1}{2}u^2)$ into the volume. This integral statement of the problem can be solved by a propagation of the discontinuity (3.4) with a speed s given by

$$s = \frac{\frac{1}{2}u_2^2 - \frac{1}{2}u_1^2}{u_2 - u_1} \tag{3.5}$$

This construction allows a solution of (3.3) integrated over fluid volumes to be found for all time. It can be shown that it is equivalent to a solution of the weak form of the equation.

$$\int \left(\phi \frac{\partial u}{\partial t} - \frac{\partial \phi}{\partial x} \cdot \tfrac{1}{2}u^2\right) dx = 0 \tag{3.6}$$

where ϕ is an arbitrary smooth function.

In order to make the solution unique, it is necessary to apply further restrictions. If, in the Riemann problem (3.4), $u_1 < u_2$, the discontinuity can still propagate with the speed (3.5). However such a solution is physically unstable since there is divergence at the shock front which would convert it into a smooth transition. A more reasonable solution in this case is

$$
\begin{aligned}
&u = u_1 \qquad x < u_1 t \\
&u = u_2 \qquad x > u_2 t \\
&u = \alpha u_1 + (1-\alpha)u_2 \qquad x = (\alpha u_1 + (1-\alpha)u_2)t \quad 0 < \alpha < 1
\end{aligned}
\tag{3.7}
$$

It can be shown that this is the solution obtained as the limit as $\epsilon \to 0$ of the problem with $\epsilon \partial^2 u/\partial x^2$ added to the right hand side. It can also be shown that (3.7) is the unique solution for which $\int u^2 \, dx$ decreases. It can then be proved that a unique solution of (3.3) is determined by the jump condition (3.5) at discontinuities and the energy condition that the total energy does not increase (Chorin and Marsden (1979)).

3.2 The shallow water equations

Consider the shallow water equations, derived from the primitive equations by vertical averaging, and assume that the variables are all independent of y.

$$
\begin{aligned}
&\frac{\partial u}{\partial t} + \frac{\partial u}{\partial x} + \frac{\partial \phi}{\partial x} - fv = 0 \\
&\frac{\partial v}{\partial t} + u\frac{\partial v}{\partial x} + fu = 0 \\
&\frac{\partial \phi}{\partial t} + \frac{\partial}{\partial x}(\phi u) = 0
\end{aligned}
\tag{3.8}
$$

The solution of this system was studied by Williams and Hori (1970). They showed that, for Rossby numbers of order unity, discontinuities in the solution tended to form in a finite time from smooth initial data. If the Rossby number is small, then the formation of discontinuities is delayed. It is an open question whether the version of (3.8) applied to a sphere with parameters appropriate to the atmosphere has smooth solutions. Sadourny (1975) found an 'energy catastrophe' in long time integrations of these equations using certain types of finite differencing which may indicate either a breakdown of smooth solutions or of those computational methods. The times involved, however, are so long as not to be physically relevant; since three dimensional processes lead to much faster breakdown. The formation of discontinuities in the one-dimensional system (3.8) may be relevant to certain mesoscale phenomena where the Rossby number is of order unity.

Once a discontinuity has been formed, equations (3.6) become meaningless, and must be replaced by the physical conservation laws from which they were derived. The conservative form, expressing conservation of mass and the two momentum components is:

$$
\frac{\partial}{\partial t}(\phi u) + \frac{\partial}{\partial x}(\phi u^2 + \tfrac{1}{2}\phi^2) - f\phi v = 0 \tag{3.9}
$$

$$\frac{\partial}{\partial t}(\phi v) + \frac{\partial}{\partial x}(\phi uv) + f\phi u = 0$$

$$\frac{\partial}{\partial t}(\phi) + \frac{\partial}{\partial x}(\phi u) = 0$$

It can again be proved that discontinuous solutions of this system can be constructed, where the speed of jump discontinuities is given by

$$S = \frac{[\phi u^2 + \tfrac{1}{2}\phi^2]}{[\phi u]} = \frac{[\phi uv]}{[\phi v]} = \frac{[\phi u]}{[\phi]} \tag{3.10}$$

where $[\ ]$ indicates a difference across the jump. (3.10) implies certain consistency conditions which have to be satisfied if a single jump is to separate two states $(\phi_1 u_1 v_1)$ and $\phi_2\ u_2\ v_2)$. These are that

$$\begin{aligned} [\phi v][\phi u^2 + \tfrac{1}{2}\phi^2] &= [\phi uv][\phi u] \\ [\phi uv][\phi] &= [\phi u][\phi v] \end{aligned} \tag{3.11}$$

which together imply that v cannot be discontinuous.

The general solution to (3.9) can be constructed by solving the Riemann problem, which is to solve (3.9) for the data

$$\begin{aligned} S_l:&\quad u = u_1\ v = v_1\ \phi = \phi_1 && x<0 \\ S_r:&\quad u = u_2\ v = v_2\ \phi = \phi_2 && x>0 \end{aligned} \tag{3.12}$$

It can be shown that the general solution for ϕ and u looks like that shown in Fig. 4, with an intermediate state S_x : $u = u_x\ \phi = \phi_x$ being generated, with one jump and one rarefaction wave separating it from S_l and S_r.

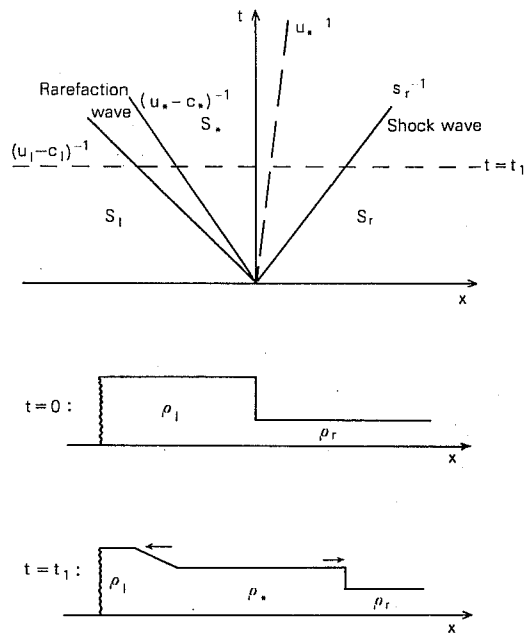

Fig. 4 Solution of the Riemann problem with initial data containing two states S_l and S_r.

The solution for v is a simple contact discontinuity, which separates the intermediate state S_* into two parts with values $(u_* \; v_1 \; \phi_*)$ and $(u_* \; v_2 \; \phi_*)$. The construction has to be carried out in such a way that characteristics converge into jumps, and diverging characteristics give rarefaction waves. If this is done, it can be proved that the total energy will decrease, and the solution agree with that obtained by adding viscous terms $\epsilon(\phi u)_{xx}$, $\epsilon(\phi v)_{xx}$ and $\epsilon\phi_{xx}$ to (3.9).

This solution can be obtained by standard centred finite differencing schemes, provided that the conservative form (3.9) is approximated, and that artificial viscosity is added which is also in conservative form. Results for the smooth initial data shown in Fig. 5 are given in Fig. 6. A jump develops in

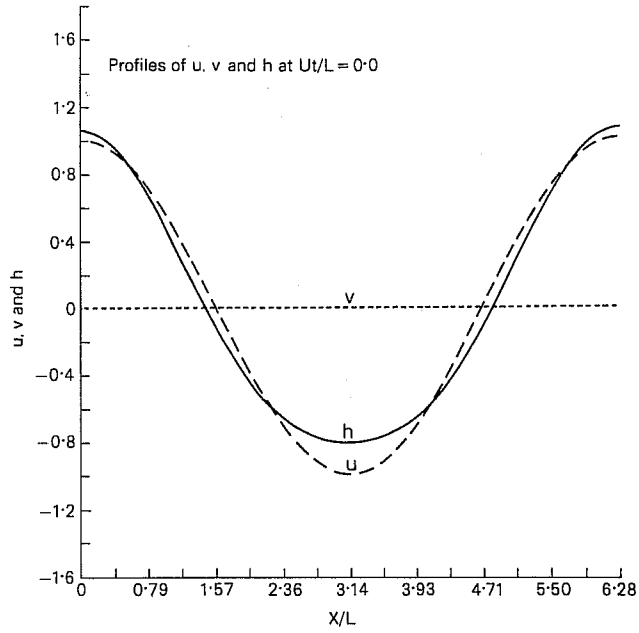

Fig. 5 Plot of ϕ, u_2 and v at t = 0

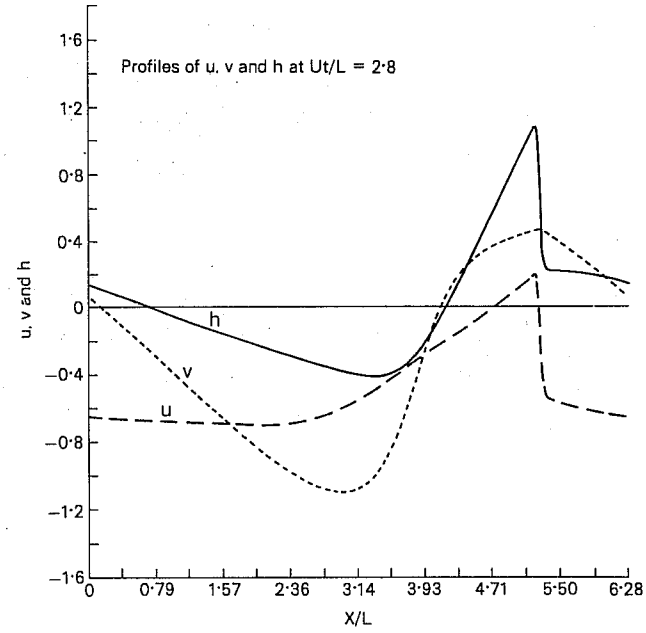

Fig. 6 Solution of equation (3.8) at $Ut/_L$ = 2.8 using conservative finite differencing.

ϕ and u, while v remains continuous. If the equations are not solved in conservation form the approximate solutions may not converge to the true solution. The results obtained using an approximation to (3.6) with artificial

viscous terms ϵu_{xx}, ϵv_{xx} and $\epsilon \phi_{xx}$ added are shown in Fig. 7. The jump propagates with the wrong speed and has the wrong height. This is because the finite difference scheme is not consistent with the conservation law (3.9) but with a different conservation law. More details of the experiments are given in Parrett and Cullen (1983).

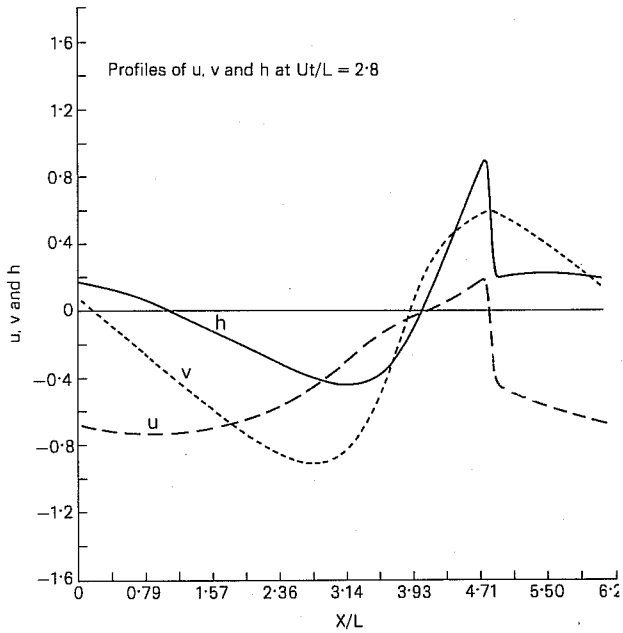

Fig. 7 Solution of equation (3.8) using non-conservative differencing.

3.3 Summary

This case is different from the incompressible equations discussed in Section 2. The inviscid differential equations no longer have smooth solutions, so the usual consistency and stability arguments are inadequate to prove convergence. We must first choose a conservation law form that expresses the correct physics, and then use a finite difference scheme consistent with that conservation law together with artificial viscosity that respects it. In general, there will be many possible conservation laws that lead to a given differential equation. The physically correct one may have to be found by experiment.

4. THE GEOSTROPHIC MOMENTUM EQUATIONS

4.1 Introduction

The scale analysis used to derive the quasi-geostrophic equations discussed in Section 2 is known to break down when locally sharp gradients occur. While vertically averaged fields, such as 500 mb contours, appear smooth, it is known that vertical cross sections of the atmosphere show sharp changes in temperature, humidity and wind. An example is the tephigram shown in Fig. 8, which is the Shanwell ascent for 12Z on 1 June 1983. There are

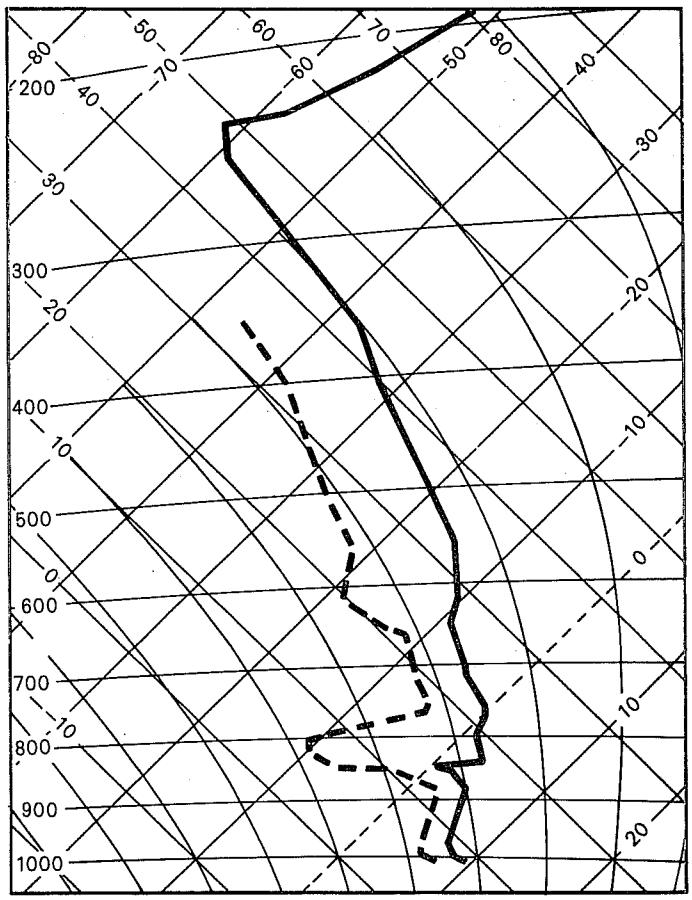

Fig. 8 Shanwell tephigram for 12Z, 1 June 1983.

at least two layers of discontinuity in the troposphere, apart from the change in temperature gradient at the tropopause. Though the scale of the transition is very small in the vertical, it is large in the horizontal, because similar jumps are visible in the tephigrams from other radiosondes taken at the same time. Quasi-geostrophic theory cannot be used to describe such a layer, but thermal wind balance can still be used by stating that the slope of any such surface is given by

$$\frac{f\,\theta_o}{g}\,\frac{[v]}{[\theta]} \qquad (4.1)$$

where [ ] represents the jump and v is the horizontal wind parallel to the surface, as was pointed out by Margules in 1892. The geostrophic momentum equations are a generalisation of quasi-geostrophic theory designed to be valid under such conditions.

4.2 Basic equations

The geostrophic momentum approximation was introduced first by Eliassen (1948) and extensively studied by Hoskins, who has reviewed the work in Hoskins (1982). It is more general than the quasi-geostrophic equations in that advection by the ageostrophic wind is included. Scaling arguments show that this provides a consistent approximation for motions where the length scale in one direction is comparable to the Rossby radius of deformation NH/f, where N is a buoyancy frequency and H a height scale; and much less than this in the cross direction. The equations take their simplest form on an f-plane, with rigid upper and lower boundaries (in pressure coordinates) and with the Boussinesq approximation made. In terms of the vertical coordinate.

$$z = \left[1 - \left(\frac{p}{p_o}\right)^{\frac{\gamma-1}{\gamma}}\right] \frac{\gamma}{\gamma-1} H_s \tag{4.2}$$

where p_o is a reference surface pressure and H_s the scale height $p_o/(\bar{\rho}_{o} g)$; the equations are

$$\begin{aligned}
&\frac{\partial u_g}{\partial t} + u\frac{\partial u_g}{\partial x} + v\frac{\partial u_g}{\partial y} + w\frac{\partial u_g}{\partial z} + \frac{\partial \phi}{\partial x} - fv = 0 \\
&\frac{\partial v_g}{\partial t} + u\frac{\partial v_g}{\partial x} + v\frac{\partial v_g}{\partial y} + w\frac{\partial u_g}{\partial z} + \frac{\partial \phi}{\partial z} + fu = 0 \\
&\frac{\partial u}{\partial x} + \frac{\partial v}{\partial y} + \frac{\partial w}{\partial z} = 0 \\
&\frac{\partial \phi}{\partial x} = fv_g, \frac{\partial \phi}{\partial y} = -fu_g, \frac{\partial \phi}{\partial z} = g\theta/\theta_o \\
&\frac{\partial \theta}{\partial t} + u\frac{\partial \theta}{\partial x} + v\frac{\partial \theta}{\partial y} + w\frac{\partial \theta}{\partial z} = 0 \\
&w = 0 \text{ at } z = 0, H
\end{aligned} \tag{4.3}$$

These equations are to be solved in a region Ω in the (x,y) plane with boundary $\partial\Omega$, or with doubly-periodic boundary conditions in (x,y). In the first case the lateral boundary conditions are

$$\underline{u} \cdot \underline{n} = 0 \text{ on } \partial\Omega \tag{4.4}$$

where $\underline{n}$ is the outward normal to $\partial\Omega$. Equations (4.3) can be written in Lagrangian conservation form (Hoskins and Draghici (1977)) by defining

$$M = v_g + fx \qquad N = -u_g + fy$$

whence

$$\frac{DN}{Dt} - f(M-fx) = 0$$

$$\frac{DM}{Dt} + f(N-fy) = 0 \qquad (4.6)$$

$$\frac{D\theta}{Dt} = 0$$

The continuity equation states that the volume, τ, of fluid elements is preserved, so that

$$\frac{D\tau}{Dt} = 0 \qquad (4.7)$$

Define

$$P = \phi + \tfrac{1}{2}f^2(x^2 + y^2) \qquad (4.8)$$

so that the consistency conditions become

$$\left(\frac{\partial P}{\partial x}, \frac{\partial P}{\partial y}, \frac{\partial P}{\partial z}\right) = (fM, fN, g\theta/\theta_o) \qquad (4.9)$$

The equations (4.6) thus determine the evolution of the gradients of the single function $P(x,y,z)$.

4.3 Two dimensional solutions

This system of equations was used by Hoskins and Bretherton (1972) to show how a discontinuity in the temperature and long-front velocity field could be formed in finite time given a basic state deformation field $\underline{u} = (-\alpha x, \alpha y, 0)$. The effect of the ageostrophic advection was to tilt the θ and M surfaces so that they met at the boundary. The equations used are the following subset of (4.6-9):

$$\frac{DM}{Dt} = -\alpha M$$

$$\frac{D\theta}{Dt} = 0 \qquad (4.10)$$

$$\frac{DA}{Dt} = -\alpha A$$

$$P = \phi + \tfrac{1}{2}f^2x^2$$

$$\left(\frac{\partial P}{\partial x}, \frac{\partial P}{\partial z}\right) = (fM, g\theta/\theta_o)$$

Since we only consider a two-dimensional cross-section, the area of an element A is used rather than the volume, τ.

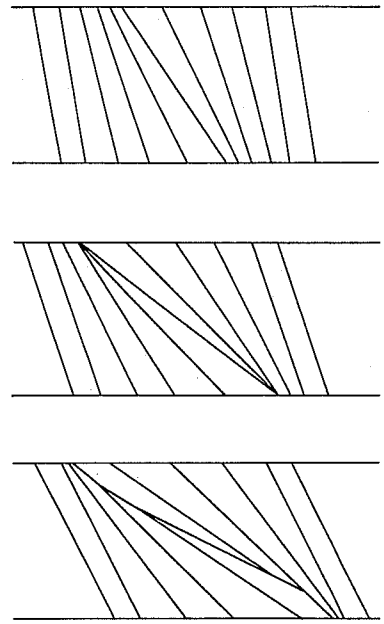

Fig. 9 Typical potential isotherms of solutions to the Hoskins-Bretherton deformation model.

The first two diagrams in Fig. 9 show the type of solutions obtained by Hoskins and Bretherton. Contours of constant M and θ are assumed to coincide in the initial data, with slopes determined by (4.1). As time goes on the values of M decrease while θ stays constant, so that the contours tilt over. Simultaneously, the areas between contours shrink. The result is that contours meet at the boundaries. After this happens, the Eulerian equations lose their validity. However, since we seek solutions with sharp interfaces between air-masses, with slopes governed by (4.1), it is reasonable to assume that the Lagrangian equations are still valid. This assumption is merely stating that the amount of fluid in a given air-mass is conserved, and its properties evolve according to (4.10). Since most fluid particles never encounter the frontal zone, it is plausible that (4.10) continues to hold almost everywhere. Solutions obtained this way can be checked for self-consistency afterwards by ensuring that no large ageostrophic accelerations are required. The term $\frac{Du_{ag}}{Dt}$ is the only term missing in (4.10) from the full primitive equations.

The third diagram in Fig. 9 shows the continuation of the solution of (4.10) after the initial frontogenesis. The front propagates into the fluid from both boundaries. The two surfaces can never meet, because of conservation of mass of intermediate fluid elements. The front is still strongest at the boundaries, in agreement with observations.

4.4 General solutions

This section gives a brief description of the general solutions of system (4.6-9). The details are given in Cullen and Purser (1983). At t = 0, assume that the volume of integration Ω is divided into n fluid elements on each of which M, N, θ and the volume τ is given. It is clear that any piecewise smooth meteorological field can be represented as accurately as desired in this way, for sufficiently large n. Write these values as

$$\{ M_i^o, N_i^o, \theta_i^o, \tau_i^o \} \quad 1 \leq i \leq n \tag{4.11}$$

At any future time, (4.5) states that

$$\theta_i = \theta_i^{(0)}$$

$$\tau_i = \tau_i^{(0)} \tag{4.12}$$

Furthermore, the equations for M_i and N_i can be completely solved given only the positions of the elements. Thus, it is sufficient to show that, given a set of values $M_i, N_i, \theta_i, \tau_i$ that there is a unique arrangement of the fluid elements satisfying (4.9). Then x and y will be determined for each element, and the equations for M_i and N_i integrated forward in time.

The problem of arranging the elements is purely geometric. A hypersurface P(x,y,z) has to be found, which is made up of hyperplanes on each of which ∇P is constant and specified as $(fM_i, fN_i, g\,\theta_i/\theta_o)$ and the volume is specified as τ_i. In order to make the surface unique, further conditions have to be specified.

It is easiest first to consider an equivalent one-dimensional problem. This is to find a curve P(x), made up of piecewise straight segments of given lengths on each of which $\frac{\partial P}{\partial x}$ is constant and specified. The curve can be constructed by joining the segments in any order. If we now add the requirement that the region in (x,s) space

$$S \geq P(x) \tag{4.13}$$

is convex, then this means that $\frac{\partial P}{\partial x}$ must be monotonically increasing in x and the order of segments is uniquely specified. Thus P(x) is uniquely determined up to an arbitrary additive constant.

In order to obtain a constraint like (4.13), recall that the geostrophic momentum approximation assumes that ageostrophic accelerations are small compared with the corresponding pressure gradient forces. If the fluid is subject to convective, inertial or symmetric instability, this assumption will clearly be invalid. Thus we must seek a solution stable to these types of perturbation. In the case of continuous solutions, the necessary condition is that the potential vorticity is non-negative. The potential vorticity q can be shown to be given by the determinant of the matrix $\underline{Q}$ where

$$Q_{ij} = \frac{\partial^2 P}{\partial x_i \partial x_j} \tag{4.14}$$

(see Hoskins (1975), Hoskins and Draghici (1977)). Thus the potential vorticity can be interpreted geometrically as the curvature of the hypersurface $P(x,y,z)$ and the condition $q \geqslant 0$ is equivalent to stating that the hyperspace of $\mathbb{R}^4$

$$S \geqslant P(x,y,z) \tag{4.15}$$

is convex.

It has been shown by Cullen and Purser (1983) that there is a unique arrangement of the fluid elements subject to condition (4.15). The mathematics required is valid in any number of dimensions. In order to illustrate the proof diagrammatically, we show it in two dimensions. The steps of the proof are shown in Fig. 10. The aim is to construct a surface $S = P(x,y)$ in (x,z,s)

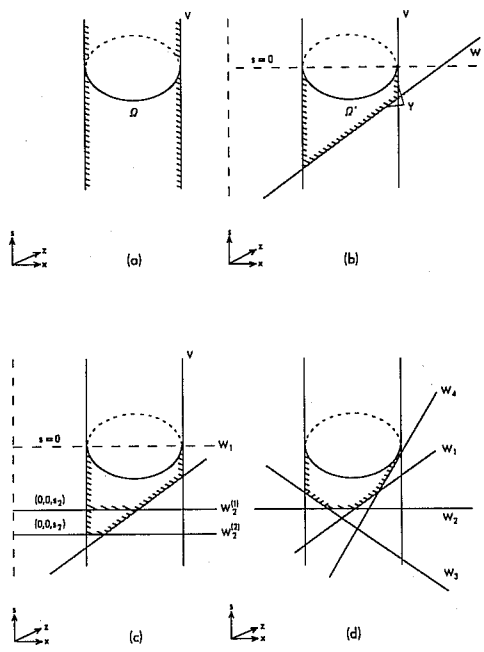

Fig. 10 Construction of solutions to the geostrophic momentum equations.

space out of an intersection of planes w_i with given slopes. The areas of the intersection of P with each w_i are also specified. In order to get the right areas the planes w_i are moved up and down in the s coordinate.

Fig. 10(a) shows the first step, which is to extend the domain Ω where the solution is required into a cylinder V in an extra dimension, measured by the coordinate s. The surface $Y = P(x,z)$ is then constructed as the intersection of this cylinder with planes w_i of specified slope, as shown in Fig. 10(b). The position of the planes is determined by their s coordinates, s_i, at $x = z = 0$, as shown in Fig. 10(c). Fig. 10(c) also shows how the areas of the intersection of Y with w_1 and w_2 varies as the position of w_2 is changed. Fig. 10(d) shows a cross section of the surface obtained by intersecting four planes with V.

In order to prove the existence of a unique surface with the correct areas for the fluid elements, we have to show that any desired combination of areas can be obtained by moving the planes w_i up and down. It is clear from Fig. 10, that as one plane is moved up and down, the area of its intersection with Y varies from zero to the whole area of Ω within a finite range of s_i. The actual proof is by iteration, making an arbitrary first guess, and then moving the plane whose area is furthest from the correct one until its area is correct, and then repeating. The convergence of this process is proved in Cullen and Purser (1983), as is the uniqueness of the solution.

4.5 Numerical solutions

Now consider the problem of obtaining the solution whose existence has been discussed in the previous section by conventional numerical techniques. For simple data it is possible to implement the construction used in the existence proof, but for practical purposes it is necessary to obtain the solution with standard finite difference methods, using Eulerian equations. Since the inviscid Eulerian equations break down at a front, artificial viscosity has to be added to represent the effects of turbulent mixing. This then leaves the question open as to whether to add viscosity to the geostrophic momentum equations or to the primitive equations. For the two dimensional case discussed in section 4.3, the alternatives can be set out as follows:

$$
\begin{aligned}
&\frac{\partial \phi}{\partial x} - fv = 0 \\
&\frac{\partial v}{\partial t} + u\frac{\partial v}{\partial x} + \alpha v + w\frac{\partial v}{\partial z} + f(\alpha x + u) = K\frac{\partial^2 v}{\partial x^2} \\
&\frac{\partial u}{\partial x} + \alpha + \frac{\partial w}{\partial z} = 0 \qquad (4.16) \\
&\frac{\partial \theta}{\partial t} + u\frac{\partial \theta}{\partial x} + w\frac{\partial \theta}{\partial z} = K\frac{\partial^2 \theta}{\partial x^2}
\end{aligned}
$$

$$\frac{\partial \phi}{\partial z} = g\theta/\theta_o$$

and:

$$\frac{\partial u}{\partial t} + u\frac{\partial u}{\partial x} + w\frac{\partial u}{\partial z} + \frac{\partial \phi}{\partial x} - fv = K\frac{\partial^2 u}{\partial x^2} \qquad (4.17)$$

in place of the first equation of (4.16). The scale analysis of Hoskins and Bretherton suggests that mixing becomes important for vorticities greater than about 10f, while the terms neglected in the geostrophic momentum equations only become important for vorticities of about 25f. This suggests the use of (4.16), since the artificial viscosity will have to be chosen to prevent the vorticity exceeding 10f. However, it is not at all clear how the solutions should be judged for physical relevance if they are different.

Numerical solution of (4.17) by standard centred difference methods is straightforward. A semi-implicit scheme must be used because of the nature of the upper and lower boundary conditions, which mean that the geopotential at $z = 0$ is determined implicitly by the requirement that

$$\int_o^H \left(\frac{\partial u}{\partial x} + \alpha\right) dz = 0 \qquad (4.18)$$

Numerical solution of (4.16) is much harder because the cross- frontal circulation is determined implicitly. Following Hoskins (1974) and others, set

$$u = -\alpha x - \frac{\partial \psi}{\partial z}$$

$$w = \frac{\partial \psi}{\partial x} \qquad (4.19)$$

where ψ is a streamfunction for the cross-frontal flow.

Then

$$\frac{g}{\theta_o}\frac{\partial \theta}{\partial z}\psi_{xx} - 2\left(f\frac{\partial v}{\partial z}\right)^2 \psi_{xz} + f\left(f + \frac{\partial v}{\partial x}\right)\psi_{zz} = Q \qquad (4.20)$$

where Q is a forcing term independent of ψ. In the presence of a front we seek solutions of (4.20) with continuous ψ but discontinuous first derivatives of ψ. It is not obvious that such a problem is well-posed, though it can be inferred to be as a result of the theorem discussed in the previous section. In the simplest case of zero potential vorticity, when constant M and θ surfaces coincide, the slopes of the constant θ lines are given by

$$S = \frac{f\theta_o}{g}\frac{dM}{d\theta} \qquad (4.21)$$

Inspection of equations (4.10) for the evolution of M and θ shows that

$$\frac{ds}{dt} = -\alpha s \tag{4.22}$$

Thus the effect of the cross-frontal circulation must be to rotate the constant θ lines according to (4.22). This means that $\partial\psi/\partial l$ is specified, where l is the direction along an isotherm, but $\partial\psi/\partial n$ is arbitrary, where n is the normal to an isotherm. The problem of finding ψ now reduces to that illustrated in Fig. 11. The problem is well posed along each isotherm that

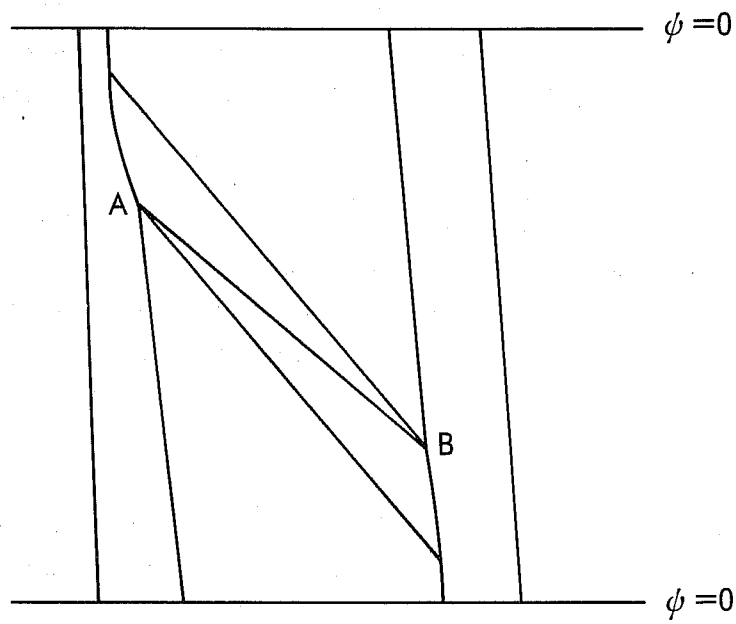

Fig. 11 Isotherms defining the solution procedure for the cross-front streamfunction equation.

intersects both boundaries, since $\partial\psi/\partial l$ and the end values of ψ are given. Where isotherms intersect the front, as at A and B, values of ψ have to be calculated at A and B using an isotherm that does reach the boundaries; and then ψ calculated along AB.

It is clear from this discussion that a direct solution for ψ, or a relaxation method designed for elliptic problems, are unlikely to work in this case. The solution presented here was obtained by iteration as follows:

a) Calculate a provisional $v_{t+\Delta t}, \theta_{t+\Delta t}$ from

$$v_{t+\Delta t} = v_t + \Delta t \left(K\frac{\partial^2 v}{\partial x^2} - \alpha v + \alpha x\frac{\partial v}{\partial x}\right) \tag{4.23}$$

$$\theta_{t+\Delta t} = \theta_t + \Delta t \left(K\frac{\partial^2\theta}{\partial x^2}\right)$$

b) Iterate, by solving the following system using a pseudo-time variable τ

$$\frac{\partial u'}{\partial \tau} + \frac{\partial \phi}{\partial x} - fv = K_1 \frac{\partial^2 u'}{\partial x^2}$$

$$\frac{\partial v}{\partial \tau} + u'\frac{\partial v}{\partial x} + w'\frac{\partial v}{\partial z} + fu' = 0$$

$$\frac{\partial u'}{\partial x} + \frac{\partial w'}{\partial z} = 0 \qquad (4.24)$$

$$\frac{\partial \theta}{\partial \tau} + u'\frac{\partial \theta}{\partial x} + w'\frac{\partial \theta}{\partial z} = 0$$

$$\frac{\partial \phi}{\partial z} = g\theta/\theta_o$$

$$w' = 0 \quad \text{at} \quad z = 0, H$$

If this iteration converges to a state with $u' = w' = 0$, it will be the desired solution of (4.16).

4.6 Results

Results for the simplest two dimensional problem described in section 4.3 are described here, with the exception that a free surface boundary condition was used. The results are therefore not exactly symmetric about $z = \frac{1}{2}H$. The initial data are

$$u = -\alpha x$$

$$v = f(X(x,z)-x) \qquad (4.25)$$

$$\theta(x,z) = \theta_o + \theta_1 \tan^{-1}\left(\frac{5X(x,z)}{L}\right)$$

where $X(x,z)$ is defined implicitly by the equation

$$\frac{x-X(x,z)}{z-\frac{1}{2}H} = \frac{-5g\theta_1}{\theta_o L f^2}\left(\frac{1}{(1+(\frac{5X(x,z)}{L})^2)}\right) \qquad (4.26)$$

and the end boundary conditions were

$$u = \mp \alpha L e^{-\alpha t} \quad \text{at} \quad x = \pm L e^{-\alpha t}$$

$$v = 0 \qquad (4.27)$$

$$\theta = \theta_o + \theta_1 \tan^{-1}(5)$$

Results are shown from three experiments at $t = 5 \times 10^4$ sec with $\alpha = 10^{-5}$ sec^{-1},

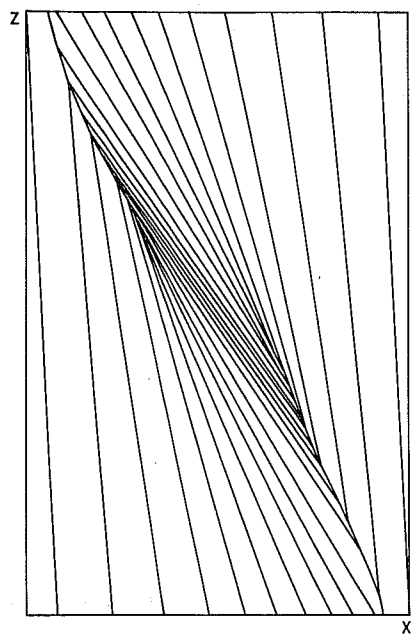

Fig. 12 Solution of equation (4.16) by explicit construction : potential temperature at $t = 5 \times 10^4$ sec.

Fig. 12 shows that obtained by explicit construction of the solution by geometric methods, with the initial data approximated by 100 segments on each of which θ and M are constant. Only the θ field is shown. Fig. 13 shows the θ field obtained by solving equation 4.17. A 200 x 20 grid was used. The results were substantically unchanged when the resolution was increased to 200 x 40. The artificial viscosity was reduced to the lowest value (1.25×10^4 $m^2 sec^{-1}$)that would allow the computation to reach this time. The discontinuity is reluctant to propagate into the fluid, as it does in Fig. 12, and close examination shows that the slopes of the isotherms disagree over a substantial area above and below the frontal surface. The associated vertical component of the cross-frontal circulation is shown in Fig. 14. The largest values are near the centre of the region.

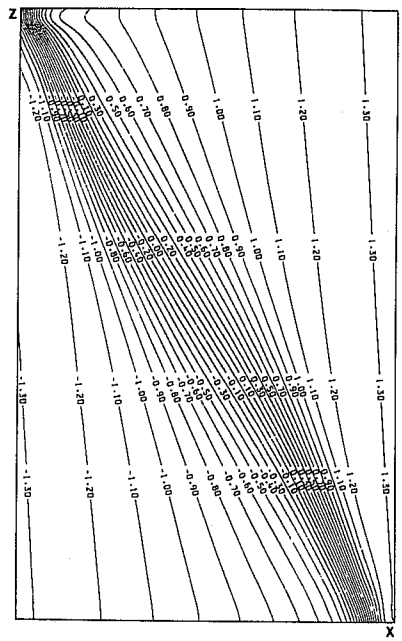

Fig. 13 Solution of equation (4.17) by by finite differences: potential temperature at $t = 5 \times 10^4$ sec.

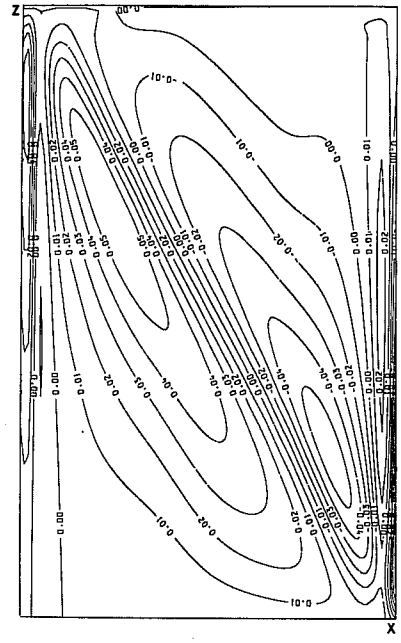

Fig. 14 As Fig. 13 : vertical velocity.

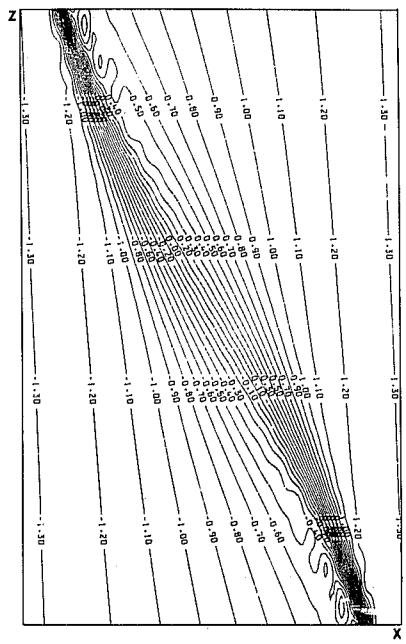

Fig. 15 Solution of equation (4.16) by finite differences : potential temperature at $t = 5 \times 10^4$ sec.

The solution obtained at the same time using equations 4.16 is shown in Fig. 15. The solution is much closer to that shown in Fig. 12, apart from the smearing in the frontal surface, where the solution is similar to Fig. 13. It was possible to use a much smaller diffusion coefficient for v and θ (600 $m^2 sec^{-1}$). The associated vertical circulation is shown in Fig. 16.

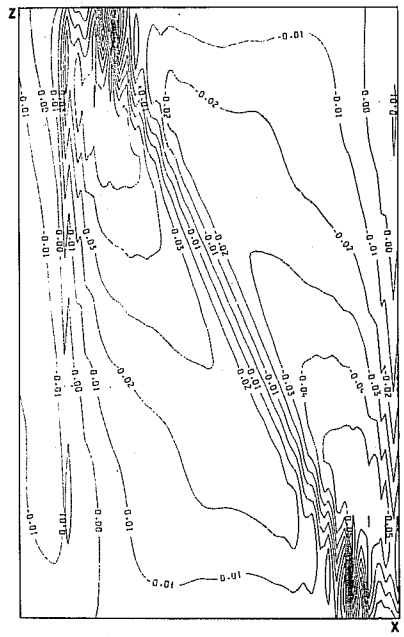

Fig. 16 As Fig. 15: vertical velocity.

The largest vertical velocities are concentrated nearer the boundaries than in Fig. 14. This is in line with observations discussed by Blumen (1980) and Ogura and Portis (1982).

Further details of these experiments are given in Cullen and Purser (1983), and examination of the differences between the solutions of (4.16) and (4.17) is continuing. Some notes on these are as follows:

a) If (4.17) is solved with different coefficients for the diffusion of u and v, the solution changes considerably. The differences resulting are as large as the difference between Figs. 13 and 15.

b) The maximum vorticities reached are 12f in Fig. 15 and 5f in Fig. 13, the minimum Richardson numbers are .08 and .2. Thus the solution in Fig. 13 should satisfy the scaling behind the geostrophic momentum approximation. However, the difference between v as calculated and v_g is about 15% near the intersection of the front with the boundary.

c) It is necessary to check that the neglected acceleration terms $\partial u/\partial t$ in the solution of (4.16) are small. Since u is calculated by iteration, a reliable $\partial u/\partial t$ has not been obtained at the time of writing.

4.7 Summary

This case is again different from those discussed in sections 2 and 3. The inviscid equations do not have smooth solutions. An inviscid solution of the geostrophic momentum equations exists, but computational evidence suggests that it is different from the inviscid limit of the primitive equations; at least in two dimensions. The latter limit does not seem to be well defined, since the solution depends on the ratio of the diffusion coefficients. The physical significance of these results is not yet clear.

5. ACKNOWLEDGEMENTS

The three-dimensional vortex calculations described in section 1 were carried out by Mrs S P Ballard. The hydraulic jump calculations and some of the frontal calculations were carried out by C A Parrett. The existence proof for the geostrophic momentum equations using convexity arguments is due to R J Purser.

6. REFERENCES

Arakawa, A. 1966. Computational design for long-term numerical integration of the equations of fluid motion: Two dimensional incompressible flow. Part I. J. Comp. Phys., 1, 119-143.

Arakawa, A. and Lamb, V.R. 1981. A potential enstrophy and energy conserving scheme for the shallow water equations. Mon. Weath. Rev., 109, 18-36.

Bennett, A.F. and Kloeden, P.E. 1981a. The quasi-geostrophic equations: approximation, predictability and equilibrium spectra of solutions. Quart. J. Roy. Meteor. Soc., 107, 121-131.

Bennett, A.F. and Kloeden, P.E. 1981b. Dissipative quasi-geostrophic motion and ocean modelling. Geophys. Astrophys. Fluid Dynam., 18, 253-262.

Blumen, W. 1980. A comparison between the Hoskins-Bretherton model of frontogenesis and the analysis of an intense surface frontal zone. J. Atmos. Sci., 37, 64-77.

Brachet, M.E., Meiron, D.I., Orszag, S.A., Nickel, B.G., Morf, R.H. and Frisch, U. 1983. Small scale structure of the Taylor-Green vortex J. Fluid Mech., 130, 411-452.

Chorin, A.J. 1981. Estimates of intermittency, spectra and blow-up in developed turbulence. Comm. Pure. Appl. Math., 34, 853-866.

Chorin. A.J. and Marsden, J.E. 1979. A mathematical introduction to fluid mechanics, Springer-Verlag.

Cullen, M.J.P. 1983. Predictability of the semi-geostrophic equations. To appear in the Proceedings of the ICDM Symposium on Predictability of Mesoscale phenomena, Hamburg, August 1983.

Cullen, M.J.P. and Purser, R.J. 1983. An extended Lagrangian theory of semi-geostrophic frontogenesis. U.K. Meteorological Office preprint.

Eliassen, A. 1948. The quasi-static equations of motion. Geofys. Publ., 17, No. 3.

Hoskins, B.J. 1974. The role of potential vorticity in symmetric stability and instability. Quart. J. Roy. Meteor. Soc., 100, 480-482.

1975. The geostrophic momentum approximation and the semi-geostrophic equations. J. Atmos. Sci., 32, 233-242.

1982. The mathematical theory of frontogenesis. Ann. Rev. Fluid Mech., 14, 131-151.

Hoskins, B.J. and Bretherton, F.P. 1972. Atmospheric frontogenesis models: mathematical formulation and solutions. J. Atmos. Sci., 29, 11-37.

Hoskins, B.J. and Draghici, I. 1977. The forcing of ageostrophic motion according to the semi-geostrophic equations and in an isentropic coordinate model. J. Atmos. Sci., 34, 1859-1867.

Judovich, V.I. 1964. A two-dimensional problem of unsteady flow of an ideal incompressible fluid across a given domain, Matem. Sbornik, 64 (106), 562-588 (English translation: 1966, Transl. Amer. Math. Soc., 57, 277-304).

Kato, T. 1967. On classical solutions of the two-dimensional non-stationary Euler equation, Arch. Rat. Mech. Anal., 25, 188-200.

Lorenz, E.N. 1979. The predictability of a flow which possesses many scales of motion, Tellus, 21, 289-307.

Ogura, Y. and Portis, D. 1982. Structure of the cold front observed in SESAME-AVE III and its comparison with the Hoskins-Bretherton frontogenesis model. J. Atmos. Sci., 39, 2773-2792.

Parrett, C.A. and Cullen, M.J.P. 1983. Simulation of atmospheric hydraulic jumps in the presence of rotation and mountains. U.K. Meteorological Office preprint.

Pedlosky, J. 1964. The stability of currents in the atmosphere and ocean, Part I, J. Atmos. Sci., 21, 201-219.

Richtmyer, R.D. and Morton, K.W. 1967. Difference methods for initial-value problems. Interscience.

Sadourny, R. 1975. The dynamics of finite difference models of the shallow water equations. J. Atmos. Sci., 32, 680-689.

Williams, R.T. and Hori, A.M. 1970. Formation of hydraulic jumps in a rotating system, J. Geophys. Res., 75, 2813-2821.